High-Pressure Preparation, Crystal Structure, and Properties of $RE_4B_6O_{15}$ (RE = Dy, Ho) with an Extension of the "Fundamental Building Block"-Descriptors

Hubert Huppertz

Department Chemie, Ludwig-Maximilians-Universität München, Butenandtstraße 5–13 (Haus D), D-81377 München, Germany

Reprint requests to Dr. H. Huppertz. E-mail: huh@cup.uni-muenchen.de

Z. Naturforsch. **58b,** 278–290 (2003); received February 11, 2003

High-pressure/high-temperature conditions of 8 GPa and 1000 °C were used to synthesize the new rare earth oxoborates $RE_4B_6O_{15}$ (RE = Dy, Ho) in a Walker-type multianvil apparatus. The single crystal X-ray structure determination of $Ho_4B_6O_{15}$ revealed the following data: $C2/c$, $a = 1164.1(1)$, $b = 436.7(1)$, $c = 1882.5(1)$ pm, $\beta = 96.71(1)°$, $Z = 4$, $R1 = 0.0291$, $wR2 = 0.0505$ (all data). The two isotypic compounds exhibit a new structure type built up from corrugated layers of BO_4 tetrahedra. In contrast to all known oxoborates the linking of the BO_4 tetrahedra is partially realized *via* common edges. Regarding the "fundamental building block"-concept, we introduce a new descriptor "⧄" for edge-sharing BO_4 tetrahedra. Temperature-resolved *in situ* powder diffraction measurements and IR/Raman-spectroscopic investigations on $Dy_4B_6O_{15}$ are also reported.

Key words: High-Pressure, Borates, Fundamental Building Block

1. Introduction

For the class of oxoborates, the numbers of synthetic studies, structural characterization, and materials processing have continuously increased during the past decade [1–4]. The structural chemistry exhibits a considerable variation that results from the ability of boron to bind to three or four oxygen atoms, forming BO_3 or BO_4 groups, which can be linked to a great structural diversity.

In this context, we are engaged in the synthesis and characterization of new rare earth oxoborates under high-pressure/high-temperature conditions. In the system RE_2O_3/B_2O_3, the rare earth oxoborates generally have the compositions RE_3BO_6 (3:1) (and thus can be regarded as orthoborates ($(RE O)_3BO_3$)), $REBO_3$ (1:1; orthoborates), and REB_3O_6 (1:3; metaborates ($RE(BO_2)_3$) [5]. Table 1 summarizes the existing compounds. While the

Table 1. Known oxoborates in the system RE_2O_3/B_2O_3.

Composition	$RE_2O_3:B_2O_3$	RE	Comments
π-$REBO_3$	1:1	Y, Ce–Nd, Sm–Lu	LT Pseudo hex. phases [11, 16]
μ-$REBO_3$	1:1	Y, Sm–Lu	HT Calcite related structure [11, 16]
λ-$REBO_3$	1:1	La–Eu	Aragonite structure [13, 22]
β-$REBO_3$	1:1	Sc, Yb, Lu	Calcite structure [14, 17–19]
ν-$REBO_3$	1:1	Ce–Nd, Sm–Dy	Triclinic (H–$NdBO_3$) [12, 15, 21]
χ-$REBO_3$	1:1	Dy, Ho, Er	Triclinic [36, 37]
H-$REBO_3$	1:1	La, Ce	Monoclinic (H–$LaBO_3$) [20, 21]
RE_3BO_6	3:1	Y, La, Pr–Lu	($(RE O)_3BO_3$) [16]
$RE_{26}(BO_3)_8O_{27}$	13:4	La	(8 La_3BO_6·La_2O_3) [31]
$RE_{17.33}(BO_3)_4(B_2O_5)_2O_{16}$	about 8.7 : 4	Y, Gd	[32, 33]
REB_3O_6	1:3	Y, La–Nd, Sm–Lu	($RE(BO_2)_3$) [23–29]
REB_5O_9	1:5	Sm–Er	Pentaborates [34]
$RE_4B_{14}O_{27}$	2:7	La	Monoclinic [35]
α-$RE_2B_4O_9$	1:2	Eu, Gd, Tb, Dy	[39]
β-$RE_2B_4O_9$	1:2	Dy	[41]
$RE_4B_6O_{15}$	2:3	Dy, Ho	[38, this work]

Abbreviations: LT low-temperature; HT high-temperature.

0932–0776/03/0400–0278 $06.00

composition of the orthoborates $RE BO_3$ [6–22] and the metaborates $RE B_3O_6$ [23–29] is beyond doubt, there exist several uncertainties concerning the rare earth borates RE_3BO_6 [5, 30]. Lin *et al.* established the crystal structures of "La_3BO_6" [31], "Y_3BO_6" [32], and "Gd_3BO_6" [33] where they found that the composition of the lanthanum compound is $La_{26}(BO_3)_8O_{27}$, showing a slight La_2O_3 excess relative to La_3BO_6 ($8\,La_3BO_6 \cdot La_2O_3$). In contrast to these results, the structure of the yttrium compound $Y_{17.33}(BO_3)_4(B_2O_5)_2O_{16}$ and the gadolinium compound $Gd_{17.33}(BO_3)_4(B_2O_5)_2O_{16}$, determined by X-ray powder diffraction data, were found to have an excess of borate. Although the Rietveld refinements resulted in reasonable residuals, some uncertainties remained. In contrast to these results, Cohen-Adad and coworkers confirmed the compositions RE_3BO_6 (RE = Y, Gd) [16]. Li *et al.* reported new pentaborates with the composition $RE B_5O_9$ (RE = Sm–Er) prepared from a decomposition reaction of $H_3RE B_6O_{12}$ at 650–700 °C [34]. Recently, Nikelski *et al.* investigated a monoclinic oxoborate with the composition $La_4B_{14}O_{27}$ possessing a network structure formed of BO_3- and BO_4-units [35].

Depending on the radius of the rare earth cation, the orthoborates $RE BO_3$ occur in several crystal structures, supplemented by a great variety of polymorphs, depending on temperature and pressure conditions. In contrast to the situation with the well described λ-, β-, ν-, and H-$RE BO_3$ orthoborates, there were numerous efforts to solve the structures of the pseudo hexagonal low temperature phases π-$RE BO_3$ (previously designated as "borates with YBO_3 structure") and the high temperature calcite related phases μ-$RE BO_3$ (also designated as "vaterite" related), but no completely acceptable solution was found [11, 16]. Recently, we were able to synthesize the new polymorphs χ-$RE BO_3$ (RE = Dy, Ho, Er), which contain layers built up from the new non-cyclic $[B_3O_9]^{9-}$-anions exhibiting one trigonal BO_3- (△) and two tetrahedral BO_4-groups (□) according to 1△2□:△2□ [36, 37].

Now, our studies focus on new compositions in the system RE_2O_3/B_2O_3 *via* multianvil high-pressure/high-temperature synthesis. Investigations were started in the system RE_2O_3/B_2O_3 with the molar ratios 1:2 and 2:3 leading to oxoborates with the new compositions $RE_2B_4O_9$ and $RE_4B_6O_{15}$ [38]. In the case of $RE_2B_4O_9$, we were able to synthesize two polymorphs, *e.g.* α-$RE_2B_4O_9$ (RE = Eu, Gd, Tb, Dy) [39, 40] and β-$RE_2B_4O_9$ (RE = Dy) [41], depending on the reaction conditions. Beside the new compositions, α-$RE_2B_4O_9$ (RE = Eu, Gd, Tb, Dy) and $RE_4B_6O_{15}$ (RE = Dy, Ho) are the first examples exhibiting edge-sharing BO_4 tetrahedra next to corner-sharing tetrahedra. In all other nearly 500 structurally characterized oxoborates, the linkage of BO_3- and BO_4-units occurs exclusively *via* corners.

Searching for oxoborates with edge-sharing BO_4 tetrahedra in the literature, we were astonished to find four other independent examples of "edge-sharing tetrahedra" as quoted in the abstracts. For the compounds $CuTm_2[B_2O_5]$ [42], $CuLn_2[B_2O_5]_2$ (Ln = Er, Lu) [43], $NiHo_2[B_2O_5]_2$ [44], and $CuHo_2[B_2O_5]_2$ [45] the authors refer to two-dimensional $[B_2O_5]^{4-}$-anions. However, none of the examples contains edge-sharing BO_4 tetrahedra. On the contrary, in all compounds there are only corner-sharing BO_4 tetrahedra. The mistake arises from the wrong translation of the German word "Ecke" into "edge" instead of "corner" in the English abstracts of those articles.

In this work, we report the synthesis, crystal structures, and properties of the compounds $RE_4B_6O_{15}$ (RE = Dy, Ho). To account for the new structural motif of edge-sharing tetrahedra, we extend the fundamental building block concept by a new descriptor. A short communication on the $Dy_4B_6O_{15}$ structure has appeared [38].

2. Experimental Section

According to eq. (1), the starting material for the synthesis of $Ho_4B_6O_{15}$ in this work was a 3:2 molar mixture of B_2O_3 (from H_3BO_3 (99.8%, Merck, Darmstadt) fired at 600 °C) with the rare earth oxide Ho_2O_3.

$$2\ Ho_2O_3 + 3\ B_2O_3 \xrightarrow[1000\ °C]{8.0\ GPa} Ho_4B_6O_{15} \qquad (1)$$

The starting material was compressed and heated *via* a multianvil assembly. Details concerning the construction of the assembly can be found in references [19] and [46–48]. For the synthesis of $Ho_4B_6O_{15}$, the assembly was compressed within 3 h to 8 GPa and heated to 1000 °C for the following 10 min. After holding this temperature for 10 min, the sample was cooled down in another

10 min. After decompression, the recovered experimental octahedron was broken apart and the sample carefully separated from the surrounding BN. $Ho_4B_6O_{15}$ was obtained as a single phase, crystalline product. The colour of $Ho_4B_6O_{15}$ depends on the light source. In daylight, $Ho_4B_6O_{15}$ has a light beige colour, while in the laboratory (neon lamps) it appears bright pink (Alexandrite-effect) [49].

For the synthesis of $Dy_4B_6O_{15}$ similar reaction conditions were used with Dy_2O_3 as starting material. Details can be found in reference [38].

3. Crystal Structure Analysis

The powder diffraction data of $RE_4B_6O_{15}$ (RE = Dy, Ho) were collected on a STOE Stadi P powder diffractometer with monochromatized Cu-K_{α_1} radiation. The diffraction patterns were indexed with the program ITO [50] on the basis of a monoclinic unit cell. The lattice parameters $a = 1167.7(2)$, $b = 437.7(1)$, $c = 1892.3(3)$ pm, $\beta = 96.72(2)°$ for $Dy_4B_6O_{15}$ and $a = 1163.8(3)$, $b = 436.5(1)$, $c = 1888.6(4)$ pm, $\beta = 96.77(3)°$ for $Ho_4B_6O_{15}$ (Table 2) were obtained from least squares fits of the powder

Table 2. Crystal data and structure refinement for $RE_4B_6O_{15}$ (RE = Dy, Ho).

Empirical formula		$Ho_4B_6O_{15}$	$Dy_4B_6O_{15}$ [38]
Molar mass [g mol^{-1}]		964.58	954.86
Crystal system		monoclinic	
Space group		$C2/c$ (No. 15)	
Powder diffractometer		STOE Stadi P	
Radiation		Cu-K_{α_1} (λ = 154.06 pm)	
a [pm]		1163.8(3)	1167.7(2)
b [pm]		436.5(1)	437.7(1)
c [pm]		1888.6(4)	1892.3(3)
β [°]		96.77(3)	96.72(2)
Volume [nm^3]		0.953(1)	0.960(2)
Single crystal diffractometer		IPDS II	
Radiation		Mo-K_α (λ = 71.073 pm)	
a [pm]		1164.1(1)	
b [pm]		436.7(1)	
c [pm]		1882.5(1)	
β [°]		96.71(1)	
Formula units per cell		$Z = 4$	
Calculated density [g cm^{-3}]		6.741	
Crystal size [mm]		0.03 × 0.03 × 0.04	
Detector distance [mm^3]		100.0	
Exposure time		8 min	
Integration Parameters	Coef. A	12.0	
	Coef. B	8.0	
	EMS	0.040	
Omega range		0–180°	
Increment		0.5°	
Absorption coefficient [mm^{-1}]		33.05	
F(000)		1672	
θ Range [°]		2 to 29	
Range in hkl		±15, ±5, ±24	
Total no. reflections		4233	
Independent reflections		1247 (R_{int} = 0.0397)	
Reflections with $I > 2\sigma$(I)		1066 (R_{sigma} = 0.0309)	
Data/parameters		1247/115	
Absorption correction		numerical (HABITUS [52])	
Transm. ratio (max/min)		0.0395/0.0997	
Goodness-of-fit on F^2		1.010	
Final R indices [$I > 2\sigma$(I)]		$R1$ = 0.0223	
		$wR2$ = 0.0487	
R Indices (all data)		$R1$ = 0.0291	
		$wR2$ = 0.0505	
Extinction coefficient		0.0036(2)	
Largest diff. peak and hole [e Å^{-3}]		2.20 and −1.25	

data. The correct indexing of the patterns was confirmed by intensity calculations [51] taking the atomic positions from the structure refinement. The lattice parameters, determined from the powder and the single crystal, agreed well (Table 2).

Small single crystals of $Ho_4B_6O_{15}$ were isolated by mechanical fragmentation and examined by Buerger precession photographs. Single crystal intensity data were collected from a regularly shaped colorless crystal (block) at room temperature by use of an IPDS II (Mo-K_α radiation (71.073 pm)). A numerical absorption correction (HABITUS [52]) was applied to the data. All relevant information concerning the data collection is listed in Table 2. The starting positional parameters were taken from the structure solution of $Dy_4B_6O_{15}$ [38]. The structure of $Ho_4B_6O_{15}$ was successfully refined with anisotropic atomic displacement parameters for all atoms using SHELXL-97 (full-matrix least-squares on F^2) [53]. Final difference Fourier syntheses revealed no significant residual peaks (see Table 2). The positional parameters and interatomic distances of the refinements are listed in the Tables 3, 4, and 5. Listings of the observed/calculated structure factors and other details are available from the Fachinformationszentrum Karlsruhe, D-76344 Eggenstein-Leopoldshafen (Germany), email: crysdata@fiz-karlsruhe.de, by quoting the registry number CSD-412041 for $Dy_4B_6O_{15}$ and CSD-412991 for $Ho_4B_6O_{15}$.

4. Results and Discussion

The structure of $RE_4B_6O_{15}$ (RE = Dy, Ho) is built up from corrugated layers of linked BO_4 tetrahedra (Fig. 1). The RE^{3+} ions are positioned between the layers. The linkage of the BO_4 tetrahedra inside the layers is realized *via* common corners as well as common edges (Fig. 6, centre). In detail, two pairs of edge-sharing tetrahedra (dark polyhedra) are linked *via* two additional corner-sharing BO_4 tetrahedra (light polyhedra) to form six-membered rings. The linkage of these rings by further corner-sharing BO_4 tetrahedra leads to rings consisting of ten BO_4 tetrahedra forming corrugated layers.

Inside the corner-sharing BO_4 tetrahedra of $Ho_4B_6O_{15}$ [$Dy_4B_6O_{15}$] the B–O bond lengths vary between 142 and 152 pm [143 and 153 pm] (Table 4). The B_2O_2 ring lies on a centre of inversion

Table 3. Atomic coordinates and U_{eq} [Å^2] for $Ho_4B_6O_{15}$ (space group $C2/c$). For comparison, the data of $Dy_4B_6O_{15}$ [38] are also listed (italics).

Atom	Wyckoff-position	x	y	z	U_{eq}
Ho1	*8f*	0.86244(2)	0.21267(2)	0.69646(2)	0.0098(1)
Dy1		*0.86202(2)*	*0.21214(4)*	*0.69642(1)*	*0.00515(6)*
Ho2	*8f*	0.13225(2)	0.20810(6)	0.59841(2)	0.0100(2)
Dy2		*0.13125(2)*	*0.20810(4)*	*0.59788(1)*	*0.00533(7)*
O1	*4e*	0	0.868(2)	¾	0.009(2)
O1		*0*	*0.8658(8)*	¾	*0.0044(6)*
O2	*8f*	0.3192	0.2391(9)	0.6388(2)	0.0104(8)
O2		*0.3185(2)*	*0.2372(6)*	*0.6380(2)*	*0.0073(5)*
O3	*8f*	0.2097(3)	0.7042(9)	0.5500(2)	0.0111(8)
O3		*0.2089(2)*	*0.7046(5)*	*0.5491(2)*	*0.0049(5)*
O4	*8f*	0.0138(3)	0.8244(9)	0.6211(2)	0.0113(8)
O4		*0.0133(2)*	*0.8246(6)*	*0.6218(2)*	*0.0064(5)*
O5	*8f*	0.9360(3)	0.4018(9)	0.8030(2)	0.0108(8)
O5		*0.9362(2)*	*0.4015(5)*	*0.8034(2)*	*0.0062(5)*
O6	*8f*	0.4152(3)	0.8735(9)	0.5695(2)	0.0116(8)
O6		*0.4151(2)*	*0.8751(6)*	*0.5695(2)*	*0.0063(5)*
O7	*8f*	0.1275(3)	0.1199(9)	0.4791(2)	0.0097(7)
O7		*0.1273(2)*	*0.1196(6)*	*0.4783(2)*	*0.0051(4)*
O8	*8f*	0.6811(4)	0.3688(9)	0.7037(2)	0.0115(8)
O8		*0.6805(2)*	*0.3654(6)*	*0.7037(2)*	*0.0067(5)*
B1	*8f*	0.0973(5)	0.296(2)	0.4129(4)	0.009(2)
B1		*0.0973(3)*	*0.2948(8)*	*0.4127(2)*	*0.0045(7)*
B2	*8f*	0.9322(5)	0.726(2)	0.8056(4)	0.011(2)
B2		*0.9335(3)*	*0.7277(9)*	*0.8059(2)*	*0.0047(7)*
B3	*8f*	0.3309(5)	0.639(2)	0.5254(4)	0.010(2)
B3		*0.3300(3)*	*0.6912(9)*	*0.5257(2)*	*0.0059(7)*

Table 4. Interatomic distances [pm] in $Ho_4B_6O_{15}$ calculated with the single crystal lattice parameters (Standard deviations in parentheses).

Ho1–O8a	223.7(4)	Ho2–O2	222.4(4)		
Ho1–O5a	224.4(4)	Ho2–O4	224.3(4)		
Ho1–O1	233.8(3)	Ho2–O5	226.6(4)		
Ho1–O2a	236.2(4)	Ho2–O7	227.4(4)		
Ho1–O5b	248.7(4)	Ho2–O8	248.7(4)		
Ho1–O8b	250.4(4)	Ho2–O3a	255.5(4)		
Ho1–O2b	256.6(4)	Ho2–O3b	258.4(4)		
Ho1–O6	263.2(4)	Ho2–O6	262.4(4)		
	Ø = 242.1		**Ø = 240.7**		
B1–O2	146.2(7)	B2–O5	141.6(7)	B3–O7	145.6(7)
B1–O7	147.0(8)	B2–O8	145.2(8)	B3–O6	144.3(7)
B1–O4	147.1(7)	B2–O4	151.1(9)	B3–O3a	151.0(8)
B1–O6	149.1(7)	B2–O1	151.6(7)	B3–O3b	153.7(7)
	Ø = 147.4		**Ø = 147.4**		**Ø = 148.7**

Table 5. Interatomic angles [°] in $Ho_4B_6O_{15}$ calculated with the single crystal lattice parameters (Standard deviations in parentheses).

O2–B1–O7	113.4(5)	O5–B2–O8	117.2(5)	O7–B3–O6	109.7(4)
O2–B1–O4	106.9(5)	O5–B2–O4	107.8(5)	O7–B3–O3a	107.1(5)
O7–B1–O4	107.0(4)	O8–B2–O4	105.2(5)	O7–B3–O3b	111.7(4)
O2–B1–O6	109.8(4)	O5–B2–O1	111.4(5)	O6–B3–O3a	119.7(5)
O7–B1–O6	109.8(5)	O8–B2–O1	106.2(5)	O6–B3–O3b	113.3(5)
O4–B1–O6	109.8(4)	O4–B2–O1	108.6(4)	O3a–B3–O3b	94.4(4)
	Ø = 109.5		**Ø = 109.4**		**Ø = 109.3**

and thus is rigorously planar. The edges of the B_2O_2 ring are slightly longer with values of 151.0(8) and 153.7(7) pm [150.7(5) and 153.3(5) pm] (Fig. 2). The average B–O distance of 147.8 pm in $RE_4B_6O_{15}$ (*RE* = Dy, Ho) is in good agreement with the average B–O bond length of 147.6 pm in simple BO_4 tetrahedra [54]. In contrast to the B···B distances between corner-sharing BO_4 tetrahedra, which cover a range of 252–262 pm, the transannular B···B distances across the B_2O_2 ring (207 pm) are markedly shorter in both compounds. O–B–O angles in corner-sharing BO_4 tetrahedra vary between 106 and 117° [107 and 116°] (Table 5). The edge-sharing tetrahedra (B3) exhibit a small and a large angle with values of 94.4(4)° and 119.7(5)° [94.1(3)° and 118.6(3)°]. The average over all angles is 109.4° in both structures.

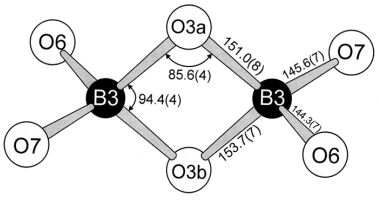

Fig. 2. Interatomic distances [pm] and angles [°] inside the edge-sharing BO_4 tetrahedra of $Ho_4B_6O_{15}$.

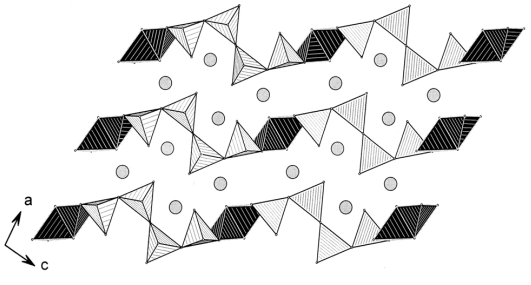

Fig. 1. Crystal structure of $RE_4B_6O_{15}$ (*RE* = Dy, Ho), view along [010]. The structure is built up from corrugated layers of corner (light) and edge-sharing (dark) BO_4 tetrahedra. The RE^{3+} ions are positioned between the layers.

In molecular chemistry, only five crystal structures containing four-membered B_2O_2 rings have been reported: $\{[HPPh_3]^+\}_2[B_4F_{10}O_2]^{2-}$ [55], the porphyrin complex $[B_2O_2(BCl_3)_2(TpClpp)]$ (TpClpp = dianion of 5,10,15,20-tetra-*p*-chlorophenyl-porphyrin) [56], the neutral diboroxane $[Me_2B–O–BMe_2]_2$ [57], 2,4-bis(2,2,6,6-tetramethylpiperidino)-1,3,2,4-dioxadiboretane [58], and the 4-oxa-3-borahomoadamantane dimer [59]. In contrast to

the tetrahedral oxygen coordination of boron in

Table 6. Interatomic distances [pm] and angles [°] in B_2O_2-rings of different molecules in comparison to the B_2O_2-ring in $Ho_4B_6O_{15}$ and $Dy_4B_6O_{15}$.

Compound	Reference	d(B–O)	d(B···B)	∠ O–B–O	∠ B–O–B
$\{[HPPh_3]^+\}_2[B_4F_{10}O_2]^{2-}$	[55]	149.8(2) 150.5(2)	210.2(3)	88.8(2)	91.2(2)
$[B_2O_2(BCl_3)_2(TpClpp)]$	[56]	150.8(12) 149.8(13)	211.9(6)	88.8(7)	91.2(7)
$[Me_2B–O–BMe_2]_2$	[57]	158.0(1)	231.1[a]	86.1(1)	93.9(1)
2,4-Bis(2,2,6,6-tetra-methylpiperidino)-1,3,2,4-dioxadiboretane	[58]	141.7(4) 141.2(4)	186.6(6)	97.5(2)	82.5(2)
4-Oxa-3-borahomoadamantane dimer	[59]	153.4(4) 155.2(4)	not mentioned	85.2(4)	94.8(4)
$Ho_4B_6O_{15}$	[this work]	151.0(8) 153.7(7)	207(1)	94.4(4)	85.6(4)
$Dy_4B_6O_{15}$	[38]	150.7(5) 153.3(5)	207.2(8)	94.1(3)	85.9(3)

[a] No standard deviation was given.

$RE_4B_6O_{15}$ (RE = Dy, Ho), none of these examples shows boron exclusively coordinated by oxygen. With the exception of the dioxadiboretane [58], the oxygen atoms in the B_2O_2 ring have a trigonal planar coordination. Table 6 gives a comparison of the interatomic distances and angles in the B_2O_2 rings of the different molecules. The B–O distances of the B_2O_2 rings of $RE_4B_6O_{15}$ (RE = Dy, Ho) are comparable to those found in $\{[HPPh_3]^+\}_2[B_4F_{10}O_2]^{2-}$ (149.8(2) and 150.5(2) pm), $[B_2O_2(BCl_3)_2(TpClpp)]$ (150.8(12) and 149.8(13) pm), and the 4-oxa-3-borahomoadamantane dimer (153.4(4) and 155.2(2) pm). Correspondingly, the B···B distances of 207 pm in $RE_4B_6O_{15}$ (RE = Dy, Ho) are comparable to the values in $\{[HPPh_3]^+\}_2[B_4F_{10}O_2]^{2-}$ (210.2(3) pm) and $[B_2O_2(BCl_3)_2(TpClpp)]$ (211.9(6) pm). In contrast, the distances in $[Me_2B–O–BMe_2]_2$ (d(B–O): 158.0(1) pm; d(B···B) 231.1 pm) and 2,4-bis-(2,2,6,6-tetramethylpiperidino)-1,3,2,4-dioxa-diboretane [d(B–O): 141.7(4) and 141.2(4) pm; d(B···B) 186.6(6) pm] show strong deviations from the average values of 151.7 pm [d(B–O)] and 209.8 pm [d(B···B)] from the former compounds. Obviously, the B_2O_2 rings are highly flexible.

In the crystal structures of $RE_4B_6O_{15}$ (RE = Dy, Ho) there are two crystallographically different RE^{3+} ions, each coordinated irregularly by eight oxygen atoms. The distances vary between 222 and 263 pm in $Ho_4B_6O_{15}$ and between 224 and 265 pm in $Dy_4B_6O_{15}$. Fig. 3 shows the coordination spheres.

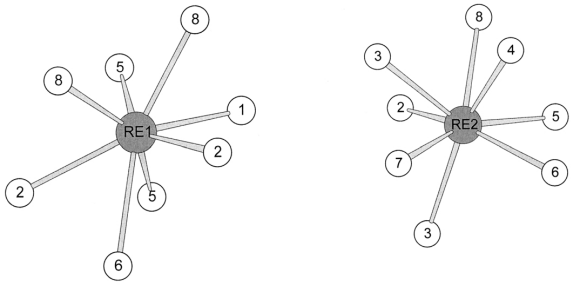

Fig. 3. Coordination spheres of RE^{3+} (grey spheres) in the crystal structures of $RE_4B_6O_{15}$ (RE = Dy, Ho).

MAPLE-values (**Ma**delung **P**art of **L**attice **E**nergy) [60–62] were calculated for $Dy_4B_6O_{15}$ ($Ho_4B_6O_{15}$) to compare the data with those of Dy_2O_3 [63] (Ho_2O_3 [64]) and the high-pressure modification B_2O_3-II [65]. For $Dy_4B_6O_{15}$ we calculated 96058 kJ/mol as compared to 96212 kJ/mol starting from the binary oxides ($2 \times Dy_2O_3$ (15199 kJ/mol) + $3 \times B_2O_3$-II (21938 kJ/mol)), a deviation of 0.2%. Calculations on $Ho_4B_6O_{15}$ led to 96116 kJ/mol compared to 96364 kJ/mol (deviation: 0.3%).

Bond-valence sums were calculated for all atoms using the bond-length/bond-strength (ΣV) [66, 67] and the CHARDI concept (**Char**ge **Di**stribution in Solids) (ΣQ) [68]. As bond-valence parameters for the former we used R_{ij} = 137.1 for B–O bonds, R_{ij} = 203.6 for Dy–O bonds, and R_{ij} = 202.5 for Ho–O bonds [67]. Table 7 gives a comparison of the charge distribution calculated with

Table 7. Charge distribution in $Dy_4B_6O_{15}$ and $Ho_4B_6O_{15}$ calculated with the bond-length/bond-strength concept (ΣV) [66,67] and the CHARDI concept (ΣQ) [68].

	Dy1	Dy2	B1	B2	B3	O1	O2	O3	O4	O5	O6	O7	O8
ΣV	+2.90	+3.10	+3.03	+3.05	+2.92	−2.22	−1.99	−1.80	−2.11	−2.20	−1.90	−2.07	−1.91
ΣQ	+2.90	+2.99	+2.98	+2.87	+3.26	−2.17	−2.04	−1.66	−2.04	−2.27	−1.84	−2.17	−1.92

	Ho1	Ho2	B1	B2	B3	O1	O2	O3	O4	O5	O6	O7	O8
ΣV	+2.93	+3.12	+3.03	+3.05	+2.94	−2.21	−2.00	−1.78	−2.09	−2.25	−1.94	−2.07	−1.93
ΣQ	+2.89	+3.00	+3.00	+2.87	+3.25	−2.14	−2.01	−1.67	−1.97	−2.31	−1.90	−2.12	−1.94

both concepts. The values confirm the formal ionic charges of Dy^{3+}, Ho^{3+}, B^{3+}, and O^{2-}.

Extension of the "Fundamental Building Block"-descriptors

The use of hierarchical sequences for organising crystal structures has long been recognized. Bragg started to classify silicate structures according to the geometry and linkage of $(Si,Al)O_4$ tetrahedra [69]. This concept was generalized by Zoltau [70] and Liebau [71]. Specifically for borate structures, there have been numerous classifications over the past decades starting with work by Edwards and Ross (1960) [72] and Christ (1960) [73]. Further developments of these concepts were performed by Tennyson (1963) [74], Ross and Edwards (1967) [75], Heller (1970) [76], and Christ and Clark (1977) [77]. Their classifications were reviewed by Christ and Clark [77]. Although the concepts were useful for small polyhedral boron units, they gave no indication about the topology or about the translation throughout the crystal structure. Units with identical numbers of $B\Phi_3$ triangles and $B\Phi_4$ tetrahedra (Φ: unspecified anion) always have identical descriptors, even where the structural arrangements are very different. The lack of topological characteristics of the linkage has been the main weakness of these notations. Therefore, a more detailed descriptor for fundamental borate building blocks that includes information on the connectivity of the BO_3 triangles and BO_4 tetrahedra was required. In the last decade, a new fundamental building block concept was introduced by Burns, Grice, and Hawthorne striking successfully a balance between the amount of information conveyed and the complexity of the descriptor [78, 79]. Although this method does not always result in a unique descriptor for the fundamental building block, considerably more information is included than in previous schemes.

The descriptor for the characterization of fundamental building blocks (FBB) proposed by Burns *et al.* [78, 79] is based on the form A:B, where A gives the specific number of BO_3 triangles (symbolized by △) and BO_4 tetrahedra (symbolized by □) in the FBB leading to the notation i△j□, where i and j are the numbers of triangles (△) and tetrahedra (□), respectively. The information on the connectivity is included in the B part of the descriptor representing a character string. This string contains the connectivity information of the polyhedra. For example adjacent △ or □ (or both) represent polyhedra that share corners. Where the polyhedra form a ring this is indicated by the delimiters <>. Sharing of polyhedra between rings is indicated by the symbols −, =, ≡, *etc.*, for one, two, three or more polyhedra, respectively. Fig. 4a gives an example for the FBB with the descriptor 1△3□:<3□>=<△2□> which contains one triangle and three tetrahedra. There are two three-membered rings of polyhedra, in which the first con-

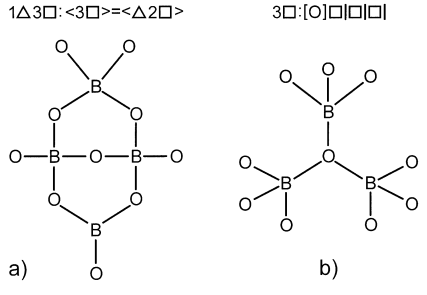

Fig. 4. Examples for the representation of fundamental building blocks in borate units with the help of descriptors after Burns *et al.* [78, 79].

tains three tetrahedra while the other one contains one triangle and two tetrahedra. Both rings have two tetrahedra in common indicated by the symbol "=". In oxoborate structures, most oxygen atoms are not bonded to more than two boron atoms. However, in some cases an oxygen atom is bonded to three (*e.g.*, tunellite ($SrB_6O_9(OH)_2 \cdot 3\,H_2O$) [80, 81]) or four boron atoms (*e.g.*, high-temperature form of boracite [82]). Therefore any anion (Φ) that is more than [2]-connected may be enclosed in the delimiters [ ] in the character string B followed by a list of polyhedra that are connected to the central unit. Each unit that is separately connected to the central unit is terminated by the symbol |, where the order of the listing is not important. For example an oxygen atom (Fig. 4b) that is shared among three BO_4 tetrahedra is represented by 3□:[O]□|□|□|. For a more detailed description the reader is referred to references [78] and [79].

The concept of Burns *et al.* [78, 79] is based on the assumption that the polymerisation of adjacent polyhedra involves only corner-sharing. As this work deals with the first oxoborates exhibiting edge-sharing BO_4 tetrahedra, the known descriptors used by Burns *et al.* have to be extended introducing a symbol for this new structural motif. For geometrical and graphical reasons (Fig. 5), we propose the new descriptor "◪" for two edge-sharing BO_4 tetrahedra. Using this symbol, the fundamental building block of $RE_4B_6O_{15}$ (RE = Dy, Ho) can be characterized by the descriptor 12□:2□◪4□◪2□ (Fig. 6, bottom). This unit is repeated only by translation to give the corrugated layer of corner- and edge-sharing BO_4 tetrahedra (Fig. 6, centre). The top of Fig. 6 has an alternative for a fundamental building block describing the layer in $RE_4B_6O_{15}$ (RE = Dy, Ho): 12□:[<□◪□◪>]2□|□|2□|□|. This formulation refers to a six-membered ring built of two pairs of edge-sharing tetrahedra linked *via* two corner-sharing BO_4 tetrahedra. This ring is decorated with six additional tetrahedra. In contrast to the former fundamental building block, this formulation captures more of the structural flavour of $RE_4B_6O_{15}$ (RE = Dy, Ho). A disadvantage of this description is the fact that next to translation also rotation of the fundamental building block has to be performed to build up the layer. There are several examples in the literature (*e.g.*: fabianite: 2△4□:<△2□>=<4□>=<△2□> [83] or brianroulstonite: 6△6□:<△□△□△□△□△□△□> [84]), where the authors [79] preferred a graphically clearer fundamental building block using the smallest possible rings instead of a unique unit, which would need only translation elements.

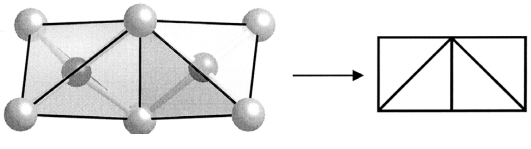

Fig. 5. The new descriptor ◪ for edge-sharing tetrahedra.

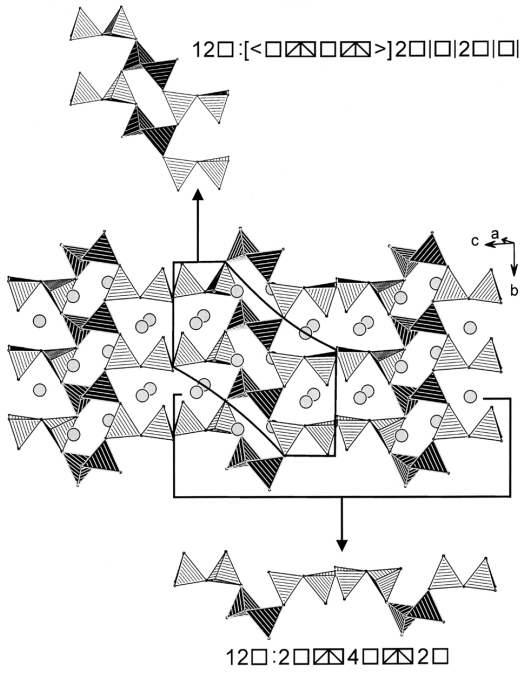

Fig. 6. View of a corrugated layer of BO_4 tetrahedra in $RE_4B_6O_{15}$ (RE = Dy, Ho). The linkage of the tetrahedra to rings is realized via common corners as well as *via* common edges.

A general description with the help of fundamental building blocks should be independent of the substance class. As $RE_4B_6O_{15}$ (RE = Dy, Ho) exhibits exclusively BO_4 tetrahedra, a classification using fundamental building units in the sense of Liebau [71] (for silicates), is an alternative. Consequently, the fundamental building block shown at the bottom of Fig. 6 represents a fundamental chain (FC) of lowest periodicity, from

which the anion can be generated by successive linkage. In terms of Liebau, this fundamental chain is an unbranched *zwölfer* chain, and the fundamental ring (FR) shown at the top of Fig. 6 represents an openbranched *sechser* ring*.

For the description of $RE_4B_6O_{15}$ (RE = Dy, Ho), we prefer 12□:2□⧄4□⧄2□ (Fig. 6, bottom), because it represents the unique fundamental building block to construct the corrugated layers of BO_4 tetrahedra by translation only.

In situ powder diffraction

To investigate the metastable character of the high-pressure phase $Dy_4B_6O_{15}$, temperature dependent measurements were performed on a STOE powder diffractometer Stadi P (Mo-K_α; λ = 71.073 pm) with a computer-controlled STOE furnace. The heating element consisted of an electrically heated graphite tube holding the sample capillary vertically with respect to the scattering plane. Bores in the graphite tube permitted unobstructed pathways for the primary beam as well as for the scattered radiation. The temperature measured by a thermocouple in the graphite tube was kept constant to within 0.2 °C. The heating rate between different temperatures was set to 22 °C/min. For temperature stabilization, a time of three minutes was allowed before start of each data acquisition. Successive heating of the metastable high-pressure phase $Dy_4B_6O_{15}$ (Fig. 7) in the range up to 800 °C led to a decomposition into the normal pressure modifications π-$DyBO_3$ and μ-$DyBO_3$ [6]. Further heating showed complete transformation into the high-temperature modification μ-$DyBO_3$ above 950 °C. Subsequent cooling gave both orthoborate phases around 600 °C followed by a complete transformation into the room temperature modification π-$DyBO_3$.

Infrared and Raman spectroscopy

The infrared (IR) spectrum of $Dy_4B_6O_{15}$ was recorded on a Bruker IFS 66v/S spectrometer scanning a range from 400 to 2000 cm^{-1}. The sample was thoroughly mixed with dried KBr (5 mg sample, 500 mg KBr) in a glove box in a dry argon atmosphere. The Raman spectrum was measured on a Dilor XY spectrometer with the help of a Raman microscope (Olympus) with an excitation wavelength of 454.5 nm on an aluminum carrier at room temperature (scanning range: 170 to 8000 cm^{-1}). In the upper range of both spectra (4000 to 2000 cm^{-1}), no vibrational bands due to OH groups or water were detectable.

* The terms "zwölfer" chain and "sechser" ring were coined by Liebau [71].

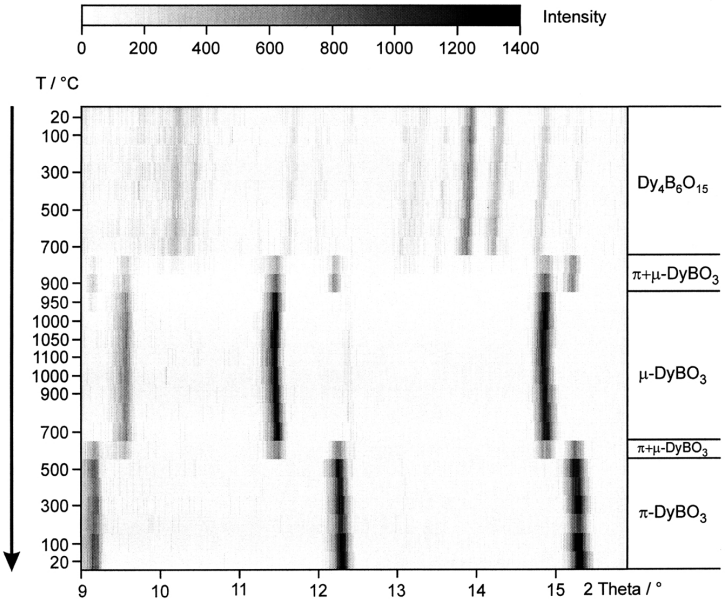

Fig. 7. Temperature dependent X-ray thermodiffractometric powder patterns (λ = 71.073 pm) of the decomposition of $Dy_4B_6O_{15}$.

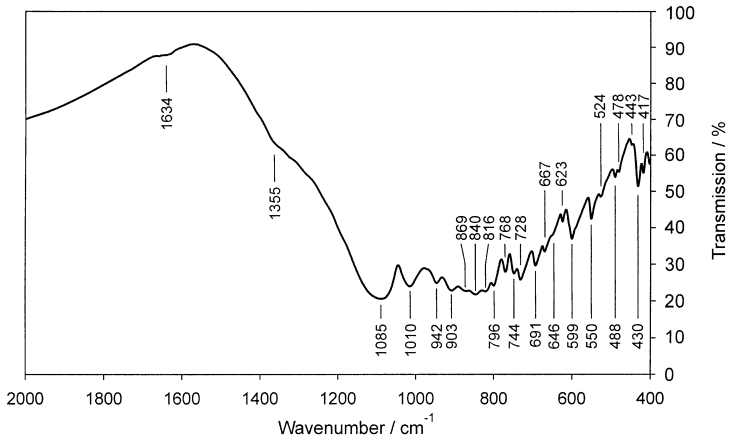

Fig. 8. Infrared spectrum of $Dy_4B_6O_{15}$.

Figures 8 and 9 show the section 400 to 2000 cm^{-1} of the infrared and Raman spectra. The spectral data of $Dy_4B_6O_{15}$ are tabulated in Table 8 in comparison to π-$GdBO_3$ [16, 85], which exhibits exclusively BO_4 tetrahedra in the form of a B_3O_9 ring. In accordance with the crystallographic data, the infrared spectrum (Fig. 8) exhibits exclusively absorptions typical for BO_4 tetrahedra. Boron, tetrahedrally coordinated to oxygen, gives rise to stretching modes in the region 1100 to 800 cm^{-1} as in π-YBO_3, π-$GdBO_3$, or $TaBO_4$ [86–88]. Bands belonging to the antisymmetric stretching mode are centred at about 1050 cm^{-1}, while the symmetric stretching mode is located in the region 850–900 cm^{-1} [89]. Due to three crystallographically independent BO_4 tetrahedra in $Dy_4B_6O_{15}$, which are corner- and edge-sharing, the stretching modes are split. Absorptions at 1085 and 1010 cm^{-1} probably correspond to antisymmetric stretching modes (1030 and 992 cm^{-1} in π-$GdBO_3$ [85]). The Raman spectrum (Fig. 9) shows the corresponding symmetrical stretching modes at 1099 and 1008 cm^{-1} (1014 and 996 cm^{-1} in π-$GdBO_3$). The symmetric stretching frequencies (ν_s) in the infrared spectrum of $Dy_4B_6O_{15}$ are in the range between 950 and 790 cm^{-1}. A sharp and strong Raman peak at 1160 cm^{-1} is unusual for oxoborates exhibiting exclusively BO_4 tetrahedra. As $Dy_4B_6O_{15}$ is the first example with edge-sharing BO_4 tetrahedra, this peak can be tentatively assigned to the symmetrical stretching mode of the B_2O_6 unit. No IR-absorption bands are observed in the range 1450–1200 cm^{-1} for $Dy_4B_6O_{15}$, as expected for oxoborates without boron in threefold oxygen coordination. On the other hand the Raman spectrum exhibits several peaks in this range, which may be

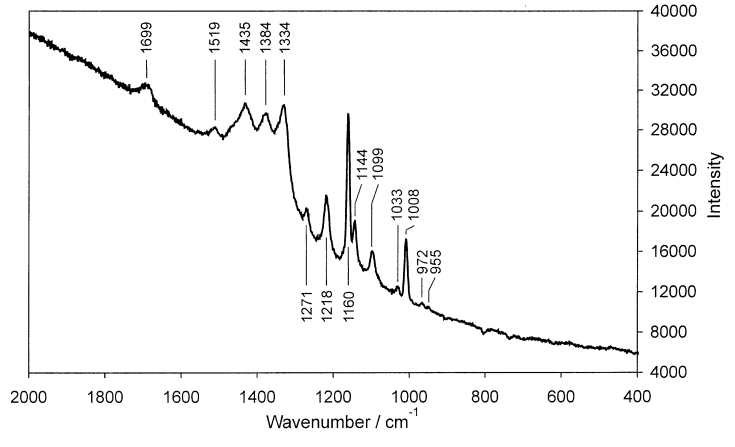

Fig. 9. Raman spectrum of $Dy_4B_6O_{15}$.

Table 8. Vibrational spectral data [cm^{-1}] in $Dy_4B_6O_{15}$ in comparison to π-$GdBO_3$ [16, 85].

$Dy_4B_6O_{15}$		π-$GdBO_3$	
IR	Raman	IR	Raman
1634 (vw, br)	1699 (w,br)		
	1519 (w)		
	1435 (s)		
1355 (vw, br)	1384 (s)		
	1334 (s)		
	1271 (w)		
	1218 (m)		
	1160 (vs)		
	1144 (m)		
1085 (vs, br) (ν_{as})	1099 (m)		
	1033 (vw)	1030 (ν_{as})	1014
1010 (s) (ν_{as})	1008 (m)	992 (ν_{as})	996
	972 (vw)		
942 (s, br)	955 (vw)		
903 (s, br)		916	
896 (br)			
840 (br)		842	
816 (br)			824
796 (w)			
768 (m)			
744 (m)		740	
728 (m)			714
691 (m)		698	
667 (m)			
646 (sh)			
623 (w)			616
599 (m)			
550 (m)			
524 (sh)			504
488 (w)			
478 (sh)			
443 (vw)			
430 (m)		422	432
417 (w)			
400 (w)		398	410

Abbreviations: s strong; vs very strong; m medium; w weak; vw very weak; br boad; sh shoulder.

associated with the new B_2O_6 unit. Spectral measurements of the phases α-$RE_2B_4O_9$ (RE = Eu, Gd, Tb, Dy) [39], with edge-sharing BO_4 tetrahedra, are in progress.

^{11}B NMR spectroscopy

The ^{11}B quadrupolar nucleus (I = 3/2) possesses a large quadrupolar moment (eQ) which couples with the local electric field gradient (eq) tensor to yield anisotropic peak shapes in the NMR spectra, which can be characterized in terms of a quadrupolar coupling constant, C_Q = (eQ)(eq)/h, and an asymmetry parameter, η, describing the relative magnitudes of the tensor components [90]. Edge-sharing of BO_4 tetrahedra should have interesting effects on the chemical shift δ. Therefore, ^{11}B solid state NMR investigations on $Dy_4B_6O_{15}$ were performed on a Bruker FT-NMR spectrometer DSX500 Avance. However, due to the paramagnetic Dy^{3+} ions the spectrum exhibited only extremely broad signals.

5. Conclusions

In this paper the structure and properties of the new rare earth oxoborates $RE_4B_6O_{15}$ (RE = Dy, Ho) synthesized *via* multianvil high-pressure synthesis from the corresponding rare earth oxides (Dy_2O_3, Ho_2O_3) and boron oxide B_2O_3 are described. These isotypic compounds are the first examples exhibiting edge-sharing BO_4 tetrahedra. To extend the framework of the FBB-concept, we introduced a new graphical descriptor "⧄" for edge-sharing BO_4 tetrahedra. The fundamental building block of $RE_4B_6O_{15}$ (RE = Dy, Ho) can be described by 12□:2□⧄4□⧄2□. *In situ* powder diffraction measurements showed that $Dy_4B_6O_{15}$ is stable up to 800 °C. Infrared and Raman spectroscopic investigations gave vibrational data, which can be tentatively assigned to the edge-sharing BO_4 tetrahedra.

Acknowledgments

H. H. gratefully acknowledges the continuous support of these investigations by Prof. Dr. W. Schnick, Department Chemie of the Ludwig-Maximilians-Universität München. Special thanks go to Prof. Dr. F. Tuczek and U. Cornelissen (Christian-Albrechts-Universität zu Kiel) for the Raman spectra, to Dr. R.-D. Hoffmann (Westfälische Wilhelms-Universität Münster) for collecting the single crystal data, to Dr. J. Senker (LMU-München) for the solid state NMR experiments, and to Dipl. Chem. S. Correll (LMU-München) for the *in situ* powder diffraction measurements. Thanks also go to Prof. Dr. F. Liebau (Christian-Albrechts-Universität zu Kiel) and Prof. P. C. Burns (University of Notre Dame, Notre Dame, Indiana) for fruitful discussions concerning the FBB-concept. For financial support, H. H. thanks the Fonds der Chemischen Industrie (FCI).

[1] P. Becker, Adv. Mater. **10**, 979 (1998).
[2] T. Sasaki, Y. Mori, M. Yoshimura, Y. K. Yap, and T. Kamimura, Mater. Sci. Eng. **30**, 1 (2000).
[3] D. A. Keszler, Curr. Opin. Solid State Mater. Sci. **1**, 204 (1996).
[4] D. A. Keszler, Curr. Opin. Solid State Mater. Sci. **4**, 155 (1999).
[5] Gmelin Handbook of Inorganic and Organometallic Chemistry **C11b**, 8th edition, Springer Verlag, Berlin (1991).
[6] E. M. Levin, R. S. Roth, and J. B. Martin, Am. Mineral. **46**, 1030 (1961).
[7] W. F. Bradley, D. L. Graf, and R. S. Roth, Acta Crystallogr. **20**, 283 (1966).
[8] J.-Y. Henry, Mater. Res. Bull. **11**, 577 (1976).
[9] R. S. Roth, J. L. Waring, and E. M. Levin, Proc. 3rd Conf. Rare Earth Res., Clearwater, Fla., 153 (1963).
[10] G. Chadeyron, M. El-Ghozzi, R. Mahiou, A. Arbus, and J. C. Cousseins, J. Solid State Chem. **128**, 261 (1997).
[11] M. Ren, J. H. Lin, Y. Dong, L. Q. Yang, M. Z. Su, and L. P. You, Chem. Mater. **11**, 1576 (1999).
[12] K. K. Palkina, V. G. Kuznetsov, L. A. Butman, and B. F. Dzhurinskii, Acad. Sci. USSR **2**, 286 (1976).
[13] H. J. Meyer, Naturwissenschaften **56**, 458 (1969).
[14] H. J. Meyer and A. Skokan, Naturwissenschaften **58**, 566 (1971).
[15] H. J. Meyer, Naturwissenschaften **59**, 215 (1972).
[16] M. Th. Cohen-Adad, O. Aloui-Lebbou, C. Goutaudier, G. Panczer, C. Dujardin, C. Pedrini, P. Florian, D. Massiot, F. Gerard, and Ch. Kappenstein, J. Solid State Chem. **154**, 204 (2000).
[17] D. A. Keszler and H. Sun, Acta Crystallogr. **C44**, 1505 (1988).
[18] S. C. Abrahams, J. L. Bernstein, and E. T. Keve, J. Appl. Crystallogr. **4**, 284 (1971).
[19] H. Huppertz, Z. Naturforsch. **56b**, 697 (2001).
[20] R. Böhlhoff, H. U. Bambauer, and W. Hoffmann, Z. Kristallogr. **133**, 386, (1971).
[21] S. Lemanceau, G. Bertrand-Chadeyron, R. Mahiou, M. El-Ghozzi, J. C. Cousseins, P. Conflant, and R. N. Vannier, J. Solid State Chem. **148**, 229 (1999).
[22] J. Weidelt and H. U. Bambauer, Naturwissenschaften **55**, 342 (1968).
[23] G. Canneri, Gazz. Chim. Ital. **56**, 450 (1926).
[24] J. Weidelt, Z. Anorg. Allg. Chem. **374**, 26 (1970).
[25] I. V. Tananaev, B. F. Dzhurinskii, and I. M. Belyakov, Izv. Akad. Nauk SSSR Neorg. Mater. **2**, 1791 (1966).
[26] H. U. Bambauer, J. Weidelt, and J. St. Ysker, Z. Kristallogr. **130**, 207 (1969).
[27] I. V. Tananaev, B. F. Dzhurinskii, and B. F. Chistova, Izv. Akad. Nauk SSSR Neorg. Mater. **11**, 165 (1975).
[28] G. D. Abdullaev, Kh. S. Mamedov, and G. D. Dzhafarov, Sov. Phys. Crystallogr. **20**, 161 (1975).
[29] C. Sieke, T. Nikelski, and Th. Schleid, Z. Anorg. Allg. Chem. **628**, 819 (2002).
[30] M. Leskelä, L. Niinistö, in K. A. Gschneider, Jr. and L. Eyring (eds.): Handbook on the Physics and Chemistry of Rare-Earth, Elsevier Science, Amsterdam (1986) p. 203.
[31] J. H. Lin, M. Z. Su, K. Wurst, and E. Schweda, J. Solid State Chem. **126**, 287 (1996).
[32] J. H. Lin, S. Zhou, L. Q. Yang, G. Q. Yao, and M. Z. Su, J. Solid State Chem. **134**, 158 (1997).
[33] J. H. Lin, L. P. You, G. X. Lu, L. Q. Yang, and M. Z. Su, J. Mater. Chem. **8**, 1051 (1998).
[34] L. Li, P. Lu, Y. Wang, X. Jin, G. Li, Y. Wang, L. You, and J. Lin, Chem. Mater. **14**, 4963 (2002).
[35] T. Nikelski and Th. Schleid, personal message.
[36] H. Huppertz and B. von der Eltz, J. Solid State Chem. **166**, 203 (2002).
[37] H. Huppertz and R.-D. Hoffmann, unpublished data.
[38] H. Huppertz and B. von der Eltz, J. Am. Chem. Soc. **124**, 9376 (2002).
[39] H. Emme and H. Huppertz, Z. Anorg. Allg. Chem. **628**, 2165 (2002).
[40] H. Emme and H. Huppertz, Chem. Eur. J. **9** (2003) in press.
[41] H. Huppertz and G. Heymann, J. Solid State Chem. (2003), in press.
[42] J. Schaefer and K. Bluhm, Z. Naturforsch. **50b**, 630 (1995).
[43] J. Schaefer and K. Bluhm, Z. Naturforsch. **50b**, 1141 (1995).
[44] K. Bluhm and A. Wiesch, Z. Naturforsch. **51b**, 677 (1996).
[45] A. Wiesch and K. Bluhm, Z. Naturforsch. **53b**, 5 (1998).
[46] D. Walker, M. A. Carpenter, and C. M. Hitch, Am. Mineral. **75**, 1020 (1990).
[47] D. Walker, Am. Mineral. **76**, 1092 (1991).
[48] D. C. Rubie, Phase Trans. **68**, 431 (1999).
[49] H. M. Farok, G. A. Saunders, W. A. Lambsom, R. Krüger, H. B. Senin, S. Bartlett, and S. Takel, Phys. Chem. Glasses **37**, 125 (1996).
[50] J. W. Visser, J. Appl. Crystallogr. **2**, 89 (1969).
[51] WinX^{POW} Software , STOE & CIE GmbH , Darmstadt (1998).
[52] W. Herrendorf and H. Bärnighausen, HABITUS, Program for Numerical Absorption Correction, University of Karlsruhe/Gießen, Germany (1993/1997).
[53] G. M. Sheldrick, SHELXL-97, Program for Crystal Structure Refinement, University of Göttingen, Germany (1997).
[54] F. C. Hawthorne, P. C. Burns, and J. D. Grice, Boron: Mineralogy, Petrology, and Geochemistry, Chapter 2, Reviews in Mineralogy 33, Mineralogical Society of America, Washington (1996).
[55] J. M. Burke, M. A. Fox, A. E. Goeta, A. K. Hughes, and T. B. Marder, Chem. Commun. 2217 (2000).
[56] W. J. Belcher, M. Breede, P. J. Brothers, and C. E. F. Rickard, Angew. Chem. **110**, 1133 (1998); Angew. Chem. Int. Ed. **37**, 1112 (1998).
[57] H. Borrmann, A. Simon, and H. Vahrenkamp, Angew. Chem. **101**, 182 (1989); Angew. Chem. Int. Ed. **28**, 180 (1989).
[58] E. Hanecker, H. Nöth, and U. Wietelmann, Chem. Ber. **119**, 1904 (1986).
[59] L. G. Vorontsova, O. S. Chizhov, L. S. Vasilev, V. V. Veselovskii, and B. M. Mikhailov, Isv. Akad. Nauk. SSSR, Ser. Khim. 353 (1981); Bull. Acad. Sci. USSR, Div. Chem. Sci. 273 (1981).
[60] R. Hoppe, Angew. Chem. **78**, 52 (1966); Angew. Chem. Int. Ed. **5**, 95 (1966).
[61] R. Hoppe, Angew. Chem. **82**, 7 (1970); Angew. Chem. Int. Ed. **9**, 25 (1970).
[62] R. Hübenthal, MAPLE, Program for the Calculation of MAPLE-Values, Vers. 4, University of Gießen (1993).

[63] W. Hase, Phys. Stat. Sol. **3**, 446 (1963).
[64] E. N. Maslen, V. A. Streltsov, and N. Ishizawa, Acta Crystallogr. **B52**, 414 (1996).
[65] C. T. Prewitt and R. D. Shannon, Acta Crystallogr. **B24**, 869 (1968).
[66] I. D. Brown and D. Altermatt, Acta Crystallogr. **B41**, 244 (1985).
[67] N. E. Brese and M. O'Keeffe, Acta Crystallogr. **B47**, 192 (1985).
[68] R. Hoppe, S. Voigt, H. Glaum, J. Kissel, H. P. Müller, and K. Bernet, J. Less-Common Met. **156**, 105 (1989).
[69] W. L. Bragg, Z. Kristallogr. **74**, 237 (1930).
[70] T. Zoltai, Am. Mineral. **45**, 960 (1960).
[71] F. Liebau, Structural Chemistry of Silicates, Springer, Berlin (1985).
[72] J. O. Edwards and V. F. Ross, J. Inorg. Nucl. Chem. **15**, 329 (1960).
[73] C. L. Christ, Am. Mineral. **45**, 334 (1960).
[74] C. Tennyson, Fortschr. Mineral. **41**, 64 (1963).
[75] V. F. Ross and J. O. Edwards, "The structural chemistry of the borates" in The Chemistry of Boron and its Compounds, Wiley, New York (1967).
[76] G. Heller, Fortschr. Chem. Forschung **15**, 206 (1970).
[77] C. L. Christ and J. R. Clark, Phys. Chem. Minerals **2**, 59 (1977).
[78] P. C. Burns, J. D. Grice, and F. C. Hawthorne, Can. Mineral. **33**, 1131 (1995).
[79] J. D. Grice and P. C. Burns, F. C. Hawthorne, Can. Mineral. **37**, 731 (1999).
[80] J. R. Clark, Am. Mineral. **49**, 1549 (1964).
[81] P. C. Burns and F. C. Hawthorne, Can. Mineral. **32**, 895 (1994).
[82] S. Sueno, J. R. Clark, J. J. Papipke, and J. A. Konnert, Am. Mineral. **58**, 691 (1973).
[83] J. A. Konnert, J. R. Clark, and C. L. Christ, Z. Kristallogr. **132**, 241 (1970).
[84] J. D. Grice, R. A. Gault, and J. van Velthuisen, Can. Mineral. **35**, 751 (1997).
[85] J. H. Denning and S. D. Ross, Spectrochim. Acta **28A**, 1775 (1972).
[86] M. Ren, J. H. Lin, Y. Dong, L. Q. Yang, M. Z. Su, and L. P. You, Chem. Mater. **11**, 1576 (1999).
[87] J. P. Laperches and P. Tarte, Spectrochim. Acta **22**, 1201 (1966).
[88] G. Blasse and G. P. M. van den Heuvel, Phys. Stat. Sol. **19**, 111 (1973).
[89] S. D. Ross, Spectrochim. Acta **28A**, 1555 (1972).
[90] S. Kroecker and J. F. Stebbins, Inorg. Chem. **40**, 6239 (2001).